

Detections of Ro-Vibrational H₂ Emission from the Disks of T Tauri Stars

Jeffrey S. Bary¹, David A. Weintraub¹ and Joel H. Kastner²

Received _____; accepted _____

Version date: November 12, 2002

¹Department of Physics & Astronomy, Vanderbilt University, P.O. Box 1807 Station B, Nashville, TN 37235; jeff.bary@vanderbilt.edu, david.a.weintraub@vanderbilt.edu

²Carlson Center for Imaging Science, RIT, 54 Lomb Memorial Drive, Rochester, NY 14623; jhkpci@cis.rit.edu

ABSTRACT

We report the detection of quiescent H_2 emission in the $v=1\rightarrow 0$ S(1) line at $2.12183\ \mu\text{m}$ in the circumstellar environment of two classical T Tauri stars, GG Tau A and LkCa 15, in high-resolution ($R \simeq 60,000$) spectra, bringing to four, including TW Hya and the weak-lined T Tauri star DoAr 21, the number of T Tauri stars showing such emission. The equivalent widths of the H_2 emission line lie in the range $0.02\text{--}0.10\ \text{\AA}$ and, in each case, the central velocity of the emission line is centered at the star’s systemic velocity. The line widths range from 9 to $14\ \text{km s}^{-1}$, in agreement with those expected from gas in Keplerian orbits in circumstellar disks surrounding K-type stars at distances $\geq 10\ \text{AU}$ from the sources. UV fluorescence and X-ray heating are likely candidate mechanisms responsible for producing the observed emission. We present mass estimates from the measured line fluxes and show that the estimated masses are consistent with those expected from the possible mechanisms responsible for stimulating the observed emission. The high temperatures and low densities required for significant emission in the $v=1\rightarrow 0$ S(1) line suggests that we have detected reservoirs of hot H_2 gas located in the low density, upper atmospheres of circumstellar disks of these stars.

Subject headings: circumstellar matter – infrared: stars – solar system: formation – stars: open clusters and associations – stars: individual (GG Tau, LkCa 15, DoAr 21, TW Hya) — stars: pre-main-sequence

1. Introduction

The study of circumstellar disks around young stars may provide insight into how and when planets form. Theoretical models suggest different mechanisms and timescales for planet formation. The core accretion model requires that a rocky core of $\sim 10M_{\oplus}$ aggregate before substantial gaseous accretion can form a Jupiter-like gas giant. This theory predicts that gas giants will form a few AU or more from the star due to the enormously greater mass of solids available beyond the snow line. A time period of roughly 10^7 yr is predicted for giant planet formation to occur through runaway accretion in a greater than minimum mass solar nebula (Lissauer 1993; Pollack et al. 1996). A second though less thoroughly investigated model, which may require a time period as brief as 10^3 yr for the formation of gas giant planets, proposes that such planets may form as a consequence of gravitational instabilities in disks (Boss 2000).

Typically, astronomers have resorted to emission from trace molecules and dust for insight into the physical conditions and masses of gas in circumstellar disks. Once these tracers disappear, the disks appear to have been removed from the system. Two decades of such observations have shown that young stellar objects (YSOs) appear to be surrounded by thick envelopes composed of dust and gas that evolve into circumstellar disks on the order of 10^6 yr (Strom et al. 1995). The absence of thermal dust emission, as measured through millimeter and infrared continuum excesses, as well as the non-detection of CO line emission towards most T Tauri stars (TTS) over the ages of 3-5 Myr old, suggests that the disks become depleted in gas and dust grains rather quickly. Two viable explanations may account for these observations: in one model, when the disk becomes undetectable it no longer exists, while in the second the disk is present but difficult to detect. According to the first of the these scenarios, circumstellar material has been dissipated through one or more of several processes: photo-evaporation, accretion onto the star, tidal stripping

by nearby stars, outflows, or strong stellar winds (Hollenbach et al. 2000). The second scenario, which describes the evolution of a circumstellar disk into a planetary system according to the core accretion theory of planet formation, suggests that larger structures (i.e., planetesimals) could have formed through accretion, collecting both solids and some gases like CO, reducing the emitting surface area of the dust and pushing the emission from both dust grains and gaseous CO below detectable levels.

In order to know whether the disks are dispersed or accretionally evolved, we must find a method to observe the part of the disk that does not disappear quickly during accretion. Since the bulk of the gaseous component of the disk, hydrogen and helium gas, will be the last to be collected into protoplanets, assuming that it avoids being removed through the various processes listed above, the H and He should remain in the disk and in the gas phase even after the dust and gaseous CO has become undetectable. Therefore, we need to study the H₂ gas directly.

H₂, at the low temperatures typically found in circumstellar environments, predominantly populates the ground vibrational level and only low rotational excitation levels and remains difficult to stimulate due to its lack of a dipole moment. In the small, inner regions of disks where temperatures may be high enough to excite H₂ gas into the first vibrational state such that 2.12183 μm emission might be possible, densities often are too high to permit detectable levels of H₂ line emission. Therefore, the bulk of the disk material has remained nearly impossible to detect directly. Assuming that most of the gas in these environments maintains a temperature much less than 1000 K, few molecules will be excited into the first vibrational state; thus, the flux of thermally excited line emission from H₂ at 2.12183 μm will be extremely low and consequently impossible to detect. In the case of T Tau, the detected emission from shocked H₂ traces approximately $10^{-7} M_{\odot}$ (Herbst et al. 1996), a mere fraction of the total mass in the system

(Weintraub et al. 1989a; Weintraub et al. 1989b; Weintraub et al. 1992).

Pure rotational H_2 line emission found in the mid-infrared at 17 and 28 μm corresponds to excitation temperatures on the order of ~ 100 K. These lines therefore should act as tracers of the bulk of the unshocked gas which resides in the circumstellar disks. Of these two lines, only the 17 μm line can be successfully observed from ground based telescopes; however, Thi et al. (1999,2001a,b) reported the detection of emission from H_2 at 17 and 28 μm using a low spatial and spectral resolution mid-infrared spectrometer on the Infrared Space Observatory (*ISO*) towards GG Tau, more evolved sources with Vega-type debris disks, and Herbig Ae/Be stars. However, in much more sensitive, higher spatial and spectral resolution mid-infrared spectra obtained by Richter et al. (2002), centered on the 17 μm H_2 emission line, no emission was observed towards GG Tau, HD 163296, and AB Aur. The Richter et al. results not only did not confirm the detections made toward these stars, but also call into question other *ISO* detections.

We have taken a different approach. Motivated by models predicting that X-rays produced by TTS may be sufficient to ionize a small fraction of the gas and indirectly stimulate observable near-infrared H_2 emission in circumstellar environments through collisions between H_2 molecules and nonthermal electrons (Gredel & Dalgarno 1995; Maloney et al. 1996; Tine et al. 1997), we have begun a study of TTS searching for near-infrared H_2 emission. We reported our initial detections of quiescent H_2 emission in the near-infrared towards TW Hya (Weintraub et al. 2000), an X-ray bright classical TTS (cTTS), and DoAr 21 (Bary et al. 2002), an X-ray bright weak-lined TTS (wTTS). We previously have suggested that the most plausible explanation for the stimulation of the H_2 emission from these sources is the X-ray ionization process. However, preliminary results from our modeling of UV and X-ray photons originating from the source and incident on the disk at varying angles (Bary, in prep) suggest that UV radiation from the source may

be an equally likely stimulus for the observed emission. Therefore, these results indicate that gaseous disks of H_2 surrounding other TTS possessing substantial X-ray and UV fluxes could be detected at $2.12183 \mu\text{m}$ using high-resolution, near-infrared spectroscopy.

In this paper, we present the first results of a high-resolution, near-infrared spectroscopic survey of cTTS and wTTS in the Taurus-Auriga and ρ Ophiuchus star forming regions. We report new detections of H_2 towards two sources: GG Tau A and LkCa 15. We use the new data and our previously reported detections of H_2 emission toward TW Hya and DoAr 21 to estimate disk masses for these four stars.

2. Observations

We obtained high-resolution ($R \simeq 60,000$), near-infrared spectra of selected TTS (Table 1) in Taurus-Auriga and ρ Ophiuchus on 1999 December 26-29, and 2000 June 20-23, UT, using the Phoenix spectrometer (Hinkle et al. 1998) on NOAO’s 4-m telescope atop Kitt Peak. In spectroscopic mode, Phoenix used a 256×1024 section of a 512×1024 Aladdin InSb detector array. Our observations were made using a $30''$ long, $0''.8$ (4 pixel) wide, north-south oriented slit, resulting in instrumental spatial and velocity resolutions of $0''.11$ and 5 km s^{-1} , respectively. Our actual seeing limited spatial resolution was $\sim 1''.4$. The spectra were centered at $2.1218 \mu\text{m}$, providing spectral coverage from 2.1167 to $2.1257 \mu\text{m}$. This spectral region includes three telluric OH lines, at 2.11766 , 2.12325 , and $2.12497 \mu\text{m}$, that provide an absolute wavelength calibration.

Integration times for our program stars, with K magnitudes $5.9 \leq K \leq 9.6$ (Table 1), ranged from 3600 s to 7200 s. Nightly observations were obtained of an A0V star, either Vega or HD 2315, for telluric calibration, with on-source integration times of 600 sec. Flat-field images were made using a tungsten filament lamp internal to Phoenix.

Observations were made by nodding the telescope 14'' along the slit, producing image pairs that were then subtracted to remove the sky background and dark current. The spectra were extracted from columns of the array covering the region from 0''7 east to 0''7 west of each source for total beam widths of 1''4, beyond which no emission was detected. Spectra were then divided by the continuum to produce normalized spectra and ratioed with that of a star with a featureless spectrum in this spectral region in order to remove telluric absorption features from the spectra of the program stars. SU Aur, a program star classified as an X-ray bright G2III wTTS produced a high signal to noise ratio, featureless spectrum and therefore, also was utilized as a telluric calibrator.

3. Results

We detected line emission very nearly at 2.12183 μm from two cTTS, GG Tau A and LkCa 15 and, as reported previously (Bary et al. 2002), the wTTS DoAr 21 and the cTTS TW Hya (Weintraub et al. 2000)³. Full spectra for all our target stars obtained with Phoenix are presented in Figure 1. Most of the absorption features in these spectra are telluric. As best as could be done given tens-of-minutes timescale fluctuations in atmospheric conditions, the spectra presented in Figure 2 have been corrected for telluric absorption features, extracted from the total spectra presented in Fig. 1 and shifted in velocity using previously measured values of V_{lsr} (Skrutskie et al. 1993; Kamazaki et al. 2001), placing the spectra in the rest frames of the stars. In no cases in which H₂ emission was observed was any emission detected in the spectra beyond 0''7 from the central positions of the star.

³Note that LkCa 15 had been classified as a wTTS (with an H α EW of 13 Å) in the Herbig Bell Catalog; however, Wolk & Walter (1996) measured $W_{\lambda}(\text{H}\alpha) = 21.9 \text{ Å}$, leading some authors to reclassify this star as a cTTS.

The central wavelengths of the emission lines were determined by fitting a Gaussian to the emission features. In each case, the central wavelength of the observed emission line matches the rest wavelength of the $2.12183\ \mu\text{m}\ v=1\rightarrow0\ S(1)$ transition of H_2 to within errors and the line is narrow ($< 14\ \text{km s}^{-1}$) yet spectrally resolved ($> 9\ \text{km s}^{-1}$). Therefore, we conclude that the observed emission is from gaseous H_2 molecules within $\sim 100\ \text{AU}$ of the stars. The central velocities of the observed H_2 reservoirs are neither red-shifted nor blue-shifted with respect to the stars and therefore experience no net line-of-sight motion. H_2 equivalent widths and line strengths for all four stars now detected in the H_2 line, corrected for extinction, are presented in Table 1, along with $3\text{-}\sigma$ upper limits for the line strengths of the non-detections. A_k was determined using previously reported values for the visual extinction (Table 5) and taking $A_k/A_v = 0.1$ (Becklin et al. 1978).

Several of our sources, notably V836 Tau, V819 Tau, and IP Tau show possible emission peaks at wavelengths just shortward of $2.122\ \mu\text{m}$. The low signal to noise levels of these stars’ spectra, however, preclude drawing any positive conclusions about these features in these data. Two absorption features centered at $2.11699\ \mu\text{m}$ and $2.12137\ \mu\text{m}$ remain after the telluric corrections were made. The line at $2.12137\ \mu\text{m}$ labeled ‘Al’ is indicated in Figure 2. The line at 2.11699 can be seen in many of the Fig. 1 spectra, in most cases slightly red-shifted to $\gtrsim 2.117\ \mu\text{m}$. We have identified these lines as photospheric absorption features produced by Al (Wallace & Hinkle 1996). Each of the stars with observed H_2 emission have both of these photospheric features, as do many of the sources not detected in H_2 emission; however, four of our sources do not. The strength of these absorption features decreases toward earlier spectral types and disappears entirely for the F and G type stars in our sample (Table 1) in agreement with the Wallace & Hinkle (1996) data.

3.1. The Location of the Emitting H₂ Gas

The spectrum of LkCa 15 is presented in Figure 2. The double-peaked H₂ emission line profile for LkCa 15 is consistent with the double-peaked CO(J=2→1) and HCO⁺ emission profiles reported by Duvert et al. (2000). The presence of blue-shifted and red-shifted emission peaks for each of these emission features, including the H₂, is indicative of gas revolving in a circumstellar disk (Beckwith & Sargent 1993; Mannings & Sargent 1997). The peak-to-peak velocity separation for the H₂ is resolved at $\Delta v \approx 10 \pm 1.5 \text{ km s}^{-1}$, which is considerably larger than the peak-to-peak separation of $\Delta v \approx 2 \text{ km s}^{-1}$ found from both the CO and HCO⁺ spectra. For a K5V star with a disk inclination angle of $34^\circ \pm 10^\circ$ as determined by Duvert et al., the H₂ emission would be produced at radial distances of between 10 and 30 AU while the CO emission should arise from molecular gas located ~ 600 AU from the source. The combination of the CO and H₂ data indicate that the near-infrared H₂ emission is sampling a different reservoir of gas than is the CO(J=2→1) emission and that the H₂ is from regions of the circumstellar disk in which gas and ice giant planets might form. In addition, the mechanism responsible for exciting the H₂ apparently is most efficient in doing so for gas at these intermediate distances from LkCa 15. As all four stars sharing H₂ emission have similar H₂ line widths, fluxes and relative velocities, it is plausible that the excitation mechanism is similar in all four stellar environments. We suggest, therefore, that the H₂ emission emerges from the 10-30 AU region around each of these four stars. Only LkCa 15, however, has a disk inclined to our line of sight such that we can distinguish the double-peaked profile (TW Hya, in fact, is known to be viewed nearly pole-on). The spatial resolution for the spectra centered on each source probes emission from the disks out to radii of ~ 30 AU for TW Hya and ~ 110 AU for LkCa 15, GG Tau, and DoAr 21. Thus, the spatial resolution in our data is consistent with our spectroscopically derived conclusion about the location of the emitting H₂.

In concluding that the gas is located in the regions 10-30 AU from the sources, we are ruling out the possibility that the emission arises in extended halos surrounding the sources. The fact that in all four cases the H₂ line emission is spatially unresolved is inconsistent with emission from a halo that should be many hundreds or thousands of AU in extent. In addition, since the H₂ emission lines appear to be spectrally resolved, the velocity line width of the gas also is inconsistent with a halo interpretation for the observed emission, for which we would expect line profiles with FWHM of only $\sim 1\text{-}2 \text{ km s}^{-1}$. Line widths of this size would be unresolved at $R \simeq 60,000$.

4. H₂ Mass Calculation

While detection of H₂ is important in establishing the continued presence of gas in the evolving circumstellar environment of TTS, a determination of the exact amount of H₂ gas still present has further reaching implications concerning the timescale for planet formation and/or the dispersal of the disk. Making such a calculation requires understanding in what environments and under what conditions the H₂ molecule can be excited into the $v = 1$, $J = 3$ state and what excitation mechanism(s) is active in this environment. The $v=1 \rightarrow 0$ S(1) transition energy corresponds to a temperature of ~ 5000 K above the ground state. Therefore, excitation temperatures between 1000 K and 2000 K typically are required in all types of astrophysical environments in order for H₂ gas to populate the first vibrationally excited level and produce detectable levels of emission at $2.12183 \mu\text{m}$ (Tanaka et al. 1989).

According to the disk model discussed in Glassgold et al. (2000), which includes X-ray heating, the *outer surface layers* of the disk may be heated to temperatures of 1000 K out to several AU, while the midplane remains cool at ~ 100 K. Hollenbach et al. (2000) show that temperatures of 1000 K produced by incident UV radiation are high enough to create photoevaporative flows that deplete disks on million year timescales. Increasing the

temperature to 2000 K would enhance the photoevaporation process, destroy the disks on even shorter timescales, and make detections of the emission we observed extremely rare or unlikely. We note that both possible stimulation mechanisms, UV fluorescence and X-ray ionization, are non-thermal processes. Consequently, the gas producing the emission may not be in Local Thermodynamic Equilibrium (LTE).

Proceeding under the assumption that the source is optically thin, we can determine the mass of H₂ emitting v=1→0 S(1) line emission from the measured line flux, independent of temperature, from

$$M(\text{H}_2)_{v=1 \rightarrow 0 \text{ S}(1)} = 1.76 \times 10^{-20} \frac{4\pi F_{if} D^2}{E_{if} A_{if}}, \quad (1)$$

where F_{if} is the line flux measured in ergs s⁻¹ cm⁻² (column 9, Table 1), E_{if} is the energy and A_{if} is the Einstein coefficient for the transition, D is the distance in pc to the source, and $M(\text{H}_2)$ is given in units of M_\odot . For the v=1→0 S(1) transition, $E_{10} = 9.338 \times 10^{-13}$ ergs and $A_{10} = 2.09 \times 10^{-7}$ s⁻¹ (Turner et al. 1977). The derived masses are given in column 2 of Table 2.

The next steps are to determine the population fraction $\chi_{v,J}(T)$, where v and J are the vibrational and rotational number for the upper level of the transition, respectively, for H₂ in the excited state located in the upper atmosphere of the disk in the 10-30 AU emission volume, and the mass fraction of the disk represented by this fractional part of the disk. One approach is to assume LTE in which case the total mass in the emitting volume of the disk would be

$$\frac{M(\text{H}_2)_{v=1 \rightarrow 0 \text{ S}(1)}}{\chi_{v,J}(T)}. \quad (2)$$

Under LTE conditions at 1500 K, $\chi_{v,J}(T) = 5.44 \times 10^{-3}$ and the masses range from

$6.4 \times 10^{-10} M_{\odot}$ for TW Hya to $8.1 \times 10^{-8} M_{\odot}$ for DoAr 21 (column 3, Table 2). If the gas is not in LTE or is at a lower temperature, then $\chi_{v,J}$ would be smaller and the masses larger. As is evident from these calculations, the masses estimated from ‘hot’ H_2 are only small fractions of the total disk masses, based on comparisons with disk gas masses estimated from observations of warm H_2 , cool dust, and cold CO (see Table 2). Since the $2.12183 \mu\text{m}$ observations of hot H_2 do not likely sample gas present in the inner disk ($r \lesssim 10 \text{ AU}$), the dense midplane of the disk at 10-30 AU, nor the disk outside of 30 AU, what is needed is a (temperature independent) scaling factor, f , such that

$$M_{disk} = f M(H_2)_{v=1 \rightarrow 0 \text{ } S(1)}. \quad (3)$$

Just as canonical scaling factors have been determined for the mass ratio between dust and gas and for the number ratio of CO and H_2 , we have calculated f from equation (3) and the “line emission” masses in Table 2 for our four stars to determine whether such a scale factor relating hot H_2 to total disk mass can be derived by using previous estimates of M_{disk} in Table 2. Scale factors derived from masses implied by several different tracers of the total disk mass are listed in Table 3. The scale factors all fall within the range from $\sim 10^7$ to $\sim 10^9$ and suggest that we are detecting as little as one billionth of the total disk mass.

The differences in these mass estimates, and therefore the range in f values, most likely arise because the various observations are sensitive to different reservoirs of material, with the (sub)mm dust continuum consistently giving the largest f values and the CO and warm H_2 smaller f values. The emission from H_2 at $2.12183 \mu\text{m}$ must arise from hot gas, at $T > 1000 \text{ K}$, which necessarily must reside near the surface of the disk and within a couple of tens of AU of the star (see §3.1 and §5), while the millimeter continuum and CO observations trace cooler gas at distances of 100s of AU. Given the location and density of the hot gas in comparison to the cool gas, it is reasonable to conclude that the tracers of

the cooler gas will uncover much more mass than the hot gas tracer.

If the hot gas is stimulated by non-thermal processes such as X-ray ionization and/or UV fluorescence, as we argue is likely in §5, the near-infrared H_2 line emission will be most sensitive to gas in the inner few tens of AU of the disk. In the case of DoAr 21 for which previous non-detections of cold dust indicated that this star was largely void of circumstellar material, our detection of quiescent H_2 emission at $2.12183\ \mu\text{m}$ suggests that a gaseous component in the inner few tens of AU of the disk persists even after the cold gas tracers stop producing detectable levels of emission (Bary et al. 2002). Therefore, we conclude that high-resolution, near-infrared spectroscopy of H_2 provides a means to detect evolved, low mass disks which may have no other observable signatures at this point in their evolution.

5. Identifying the Stimulation Mechanism

H_2 emission in the near-infrared has been observed in a variety of stellar environments such as planetary nebulae, Herbig-Haro objects, and galaxies. For example, H_2 emission observed from planetary nebulae and HH objects is attributed to heating of molecular gas as it encounters shock fronts from outflows associated with the source. UV radiation produced in accretion flows or emitted by the sub-dwarf embedded in a PN can likewise stimulate H_2 molecules located near these sources to fluoresce. Near-infrared H_2 emission also has been observed towards a Seyfert galaxy, with X-rays suggested as the mechanism responsible for the excitation of the molecules (Tine et al. 1997). Similarly, several authors have proposed that gas densities and X-ray luminosities in the environments of TTS also are sufficient to produce H_2 emission in the near-infrared, with the strongest transition being the $v=1\rightarrow0$ S(1) ro-vibration line (Gredel & Dalgarno 1995; Maloney et al. 1996; Tine et al. 1997).

With the high-resolution velocity information from our data placing the velocity of

the gas at the systemic velocities of the stars with only a very small dispersion, and the spatial resolution of and spectral information from our data placing the H_2 emission within a few tens of AU of the respective stars, we conclude that the observed emission is unlikely to originate from shock excitation in a YSO outflow, for which typical outflow velocities are at least many tens of km s^{-1} and the shocked gas is most often observed at great distances from the stars. The FWHM velocity distribution for the observed emission lines, ~ 9 to 14 km s^{-1} , is larger than the thermal broadening expected from H_2 , but not large enough to be produced by gas shocked by a jet, even for a jet aligned perpendicular to the line of sight with a small opening angle. For example, assuming an extremely small opening angle of $\sim 4^\circ$, as has been observed for the outflow observed towards RW Aur (Dougados et al. 2000), and a launch velocity of $\sim 200 \text{ km s}^{-1}$, the H_2 line would be broadened by $\simeq 10 \text{ km s}^{-1}$. Even a tiny inclination angle of the jet toward our line of sight would increase the breadth of the line tremendously by creating blue- and red-shifted jets of gas. Since all of our sources’ emission lines have similarly small FWHM, it is statistically reasonable to argue that most of these sources do not possess jets aligned nearly perpendicular to the line of sight, although conceivably one of the sources might be so aligned. Therefore, we conclude that shock excitation in a stellar outflow is not likely to be the stimulating mechanism for most and probably not any of these sources.

Since the observed line widths appear to rule out shocks in outflowing gas, the velocity dispersion in our line must be due only to thermal and/or orbital broadening, leaving ultraviolet pumping and X-ray ionization as candidate mechanisms for stimulating the H_2 emission. Ultraviolet pumping and X-ray ionization would serve to enhance the population of H_2 molecules in excited states in the circumstellar disks of young stars via photon excitation (UV) or secondary interactions between H_2 molecules and ions produced by X-ray ionization events. Using the disk model found in Glassgold et al. (2000) and cross-sections for H_2 molecules as “seen” by UV photons and X-rays determined from Yan

et al. (1998) we have calculated a set of optical depth surfaces in the disk, in the range $0.2 \leq \tau \leq 2$, to which photons of different energies and angles incident upon the inner disk would penetrate. The optical depth surfaces determined by our model assume a disk composed entirely of H_2 molecules with incident photons originating at an inner radius of 0.35 AU. Although this model is simple, the results from our preliminary simulations (Bary, in prep) suggest that both UV and X-ray photons could be responsible for the observed $2.1218 \mu\text{m}$ emission. Because the interaction cross-sections for the X-rays are much smaller than those for UV photons, X-rays will penetrate through a greater optical column than will UV photons. Thus, some X-ray photons will penetrate deeper below the surface layer of the disk than will the UV photons and deposit their energy in regions of the disk in which the number densities are greater than 10^7 cm^{-3} ; such densities are too high to produce the observed H_2 emission at radii less than 50 AU. At these densities, excited H_2 molecules will be collisionally de-excited. However, a significant fraction of the X-ray photons will be absorbed at the more shallow disk layers where the number density is below 10^7 cm^{-3} . The fraction of X-ray photons absorbed in regions of greater vs. smaller number density will depend on the exact physical shape (flaring profile) of the disk, the vertical density gradient in the disk, and the place of origin of the X-ray photons (stellar surface or accretion funnels). A majority of UV photons incident upon the surface of the disk at distances between 10 and 30 AU will be absorbed at distances of 5-10 AU above the mid-plane, in a region of the disk where the number densities ($10^4 \leq n \leq 10^7 \text{ cm}^{-3}$) are suitable for producing observable H_2 emission at $2.12183 \mu\text{m}$.

Because both UV and X-ray photons are capable of penetrating to and being absorbed at depths and radii at which the observed line emission likely arises, in the following discussion, we examine both UV fluorescence and X-ray excitation models to determine if the flux of emission observed towards each source can be stimulated by either or both mechanisms.

5.1. X-ray Stimulated Emission

We now predict the flux of the $v=1 \rightarrow 0$ S(1) line emission using the models of X-ray excitation presented by Maloney et al. (1996). For example, using the ROSAT measured X-ray flux from DoAr 21, we determined the X-ray energy deposition rate per volume element H_x/n to be 3.8×10^{-27} ergs s^{-1} cm^{-3} at a distance of 10 AU from the source in a disk and assuming a number density⁴ of 10^5 cm^{-3} . For this range in likely values of H_x/n , we can estimate the emergent integrated surface brightness in the $1 \rightarrow 0$ S(1) emission line from Figure 6a of Maloney et al. (1996). Assuming the emission emerges from an annulus in a circumstellar disk stretching from 10 to 30 AU and at a distance of 160 pc, the predicted flux of the $1 \rightarrow 0$ S(1) line lies in the range 2.4×10^{-17} to 2.4×10^{-14} ergs s^{-1} cm^{-2} (Table 4). The observed line flux falls within and near the top of this predicted range. Thus, this calculation suggests that the observed emission could be attributed solely to X-ray excitation. Similar results (Table 4) are found using the X-ray fluxes for GG Tau, TW Hya, and using an assumed X-ray flux for LkCa 15.

Thus, for the stars that are sources of X-rays, we have determined that X-rays are capable of stimulating the observed H_2 emission at $2.12183 \mu m$. In fact, two of the four sources for which we have detected the quiescent H_2 emission, DoAr 21 and TW Hya, are among the X-ray brightest TTS (column 6, Table 1). However, GG Tau is considerably less X-ray luminous, while LkCa 15 was not detected at all by ROSAT. If X-rays are important for stimulating the observed emission, we must understand why these four stars appear so

⁴Note that this density is below the critical density and all of the H_2 line flux predicted to be stimulated by the X-rays will be observable. However, even if far less than 50% of the X-rays are absorbed in a less than critically dense region and the predicted line fluxes are cut in half, the X-ray mechanism still proves to be effective at producing most of the observed H_2 emission from these sources.

different in observed X-ray emission.

Historically, we know that most wTTS are strong X-ray emitters, with many wTTS having been discovered through extensive X-ray surveys of star forming regions (e.g., Casanova et al. 1995; Neuhäuser et al. 1995). The apparent bimodal distribution of TTS as X-ray sources, in which wTTS were almost always detected and cTTS were much less often detected, led to widespread acceptance that the X-ray emission mechanism was related to the evolution of the star/disk system. According to this scenario, X-ray emission from wTTS is attributed to conservation of angular momentum and “spinning up” of the star as the magnetic field lines decouple from the dissipating circumstellar disk, allowing the forming star to contract (Edwards et al. 1993; Bouvier et al. 1993). With the decrease in rotational period of the source, surface magnetic activity presumably increases. In turn, this process is expected to lead to an increase in coronal heating and the production of detectable levels of X-ray emission. Thus for several years, X-ray emission was thought to distinguish wTTS from cTTS, with observational evidence suggesting that wTTS were, indeed, fast rotators (Choi & Herbst 1996; Shevchenko & Herbst 1998) while cTTS rotated more slowly due to disk-locking and therefore lacked the mechanism for X-ray production. With increasing statistics from large X-ray surveys, however, many cTTS also have been found to be generating X-rays. Since X-rays are no longer thought to distinguish cTTS from wTTS (Feigelson & Montmerle 1999), it is no longer clear what mechanism produces X-rays in the YSO environment. In addition, increasing evidence has called into question the existence of a bimodal rotation period distribution for wTTS and cTTS (Stassun et al. 1999; Rebull et al. 2001), with some authors now suggesting such a distribution applies only to TTS in the mass range of about 0.25-1.0 M_{\odot} (Herbst 2002).

In recent work based on Chandra spectra, Kastner et al. (2002) use the inferred plasma temperature distribution and the relative densities of iron, oxygen and neon deduced from

high-resolution Chandra X-ray spectroscopy to infer that the bulk of the X-ray emission from TW Hya is generated via mass accretion from its circumstellar disk. If this is correct, and more so if this is a common mechanism for X-ray production, then X-ray bright TTS — including wTTS — would be those still accreting material from their disks. This interpretation is contrary to the common wisdom suggesting X-rays are dominantly from fast rotating wTTS that are no longer accreting material from circumstellar disks and suggests that DoAr 21, despite being a wTTS, not only has H_2 in a circumstellar disk, but may still be actively accreting material from a circumstellar disk (Bary et al. 2002).

We suggest that despite the absence of detectable levels of X-ray emission, LkCa 15 could be accreting from a circumstellar disk; however, because its thick disk is oriented nearly along our line of sight, the disk may absorb a significant fraction of the X-ray emission, thereby decreasing the X-ray flux that escapes the circumstellar region to a level that is below detection thresholds. A column of 10^{21} cm^{-2} (equivalent to $A_v \sim 0.5$; $A_v \sim 0.64$ for LkCa 15 (see Table 5)) is sufficient to decrease the flux from a source with an intrinsic X-ray luminosity of $L_x = 3 \times 10^{29} \text{ ergs s}^{-1}$ to a count rate below 0.003 s^{-1} , which is well below the detection threshold of the ROSAT all sky survey. A scenario such as this may explain the observed differences in X-ray fluxes from cTTS and wTTS, since most cTTS are observed to have thicker disks more capable of attenuating the flux of X-rays produced within the inner boundary of the disks.

A star that previously has stood out as a notable exception to the absence of X-ray bright cTTS is TW Hya. TW Hya has been imaged extensively at wavelengths ranging from the optical (Krist et al. 2000) and near-infrared (Weinberger et al. 2002) through the mm (Wilner et al. 2000), and all of these observations indicate the presence of a face-on disk. Therefore, in the case of TW Hya, there is no line-of-sight gas and dust associated with the circumstellar disk of the star to attenuate the X-ray emission from the star.

5.2. Ultraviolet Stimulated Emission

In an attempt to determine whether that the UV flux (F_{UV}) is capable of producing the observed H_2 line flux, we compare observed and extrapolated values of F_{UV} with those predicted from the models of Black and van Dishoeck (1987). Using the model for UV fluorescence found in Black and van Dishoeck (1987), the predicted UV flux is given by

$$F_{\text{UV}} = \frac{4\pi F_{\text{v}=1\rightarrow0 \text{ S}(1)}}{\Omega_{\text{Disk}} \varepsilon f_{1\rightarrow0}}, \quad (4)$$

where ε is the UV absorption efficiency, $f_{1\rightarrow0}$ is the fraction of the total infrared flux emitted in the the 2.12183 μm emission line, Ω_{Disk} is the solid angle of the disk that intercepts the stellar UV flux and $F_{\text{v}=1\rightarrow0 \text{ S}(1)}$ is the observed H_2 line flux in $\text{erg s}^{-1} \text{ cm}^{-2}$. Using the scale height of the disk at a distance of 30 AU from the source, we conservatively estimate $\frac{\Omega_{\text{Disk}}}{4\pi}$ to be ≈ 0.1 since UV photons are likely to be absorbed at distances above the midplane that are larger than the scale height. The model dependent UV absorption efficiencies and line fractions were chosen from models 12 and 15 from Black and van Dishoeck (1987) to provide a wide range of predicted UV fluxes.

Of the four sources, TW Hya is the only star that has been observed in the wavelength range, 925-1130 Å, which are the wavelengths of interest because only photons with $\lambda \leq 1130 \text{ Å}$ possess the right energy to produce infrared H_2 fluorescent emission. Far Ultraviolet Space Explorer *FUSE* observations (Herczeg, private communication) show that the uncorrected line and continuum fluxes for TW Hya have nearly the same magnitude when integrated over the wavelengths 925-1130 Å. Using equation (4), we predict a range of $6.6 \times 10^{-12} \leq F_{\text{UV}} \leq 4.8 \times 10^{-10} \text{ erg s}^{-1} \text{ cm}^{-2}$ for the value of UV flux from TW Hya necessary to stimulate the observed H_2 line emission. Using the sum of the integrated *FUSE* continuum flux and the line fluxes (CIII at 977 Å, O VIII at 1032 and 1038 Å) for TW Hya

we estimate that the model dependent UV flux is responsible for 1% to 20% of the observed H_2 line emission at $2.12183 \mu\text{m}$.

For the other sources, we converted the U magnitude for each star to a flux at 3620 \AA . Assuming the stars radiate as blackbodies with temperatures indicated by their main-sequence spectral types, we extrapolated the 3620 \AA flux to 1000 \AA . By comparing the theoretical F_{UV} for TW Hya to the observed value of F_{UV} , we can determine if the extrapolation method accurately predicts the UV continuum flux. For TW Hya, we determined F_{UV} to be about $3 \times 10^{-18} \text{ erg s}^{-1} \text{ cm}^{-2}$, about five orders of magnitude less than the level observed by *FUSE*. We conclude that the extrapolation method for determining F_{UV} is a poor predictor of the stellar UV flux. Therefore, for DoAr 21, LkCa 15, and GG Tau, without *FUSE* observations we can only surmise that their F_{UV} spectra may be similar to that of TW Hya and, thus, that their actual levels of F_{UV} may be capable of stimulating at least part of the observed $2.12183 \mu\text{m}$ line emission.

The results of the UV fluorescence model suggest that a significant fraction of the infrared H_2 emission may be produced via UV photo-excitation for each star. However, the model is not well constrained. For example, UV emission can be absorbed by circumstellar and interstellar gas, in which case, the UV line and continuum fluxes would be lower limits. Predicting the UV flux necessary to produce the $2.12183 \mu\text{m}$ line flux is complicated by the narrow range of densities for which the efficiencies and line fractions have been calculated. In addition, Black and van Dishoeck (1987) assume a plane parallel cloud of gas with a constant density; in our case we used $3 \times 10^3 \text{ cm}^{-3}$, while in a realistic circumstellar disk there will be a density gradient with the outer layers of the disk having lower densities and the inner layers of the disk having much higher densities. As shown in Black and van Dishoeck (1987), the efficiencies can be affected greatly by the column and space densities of the gas.

Ultraviolet excesses associated with pre-main-sequence stars normally are attributed to active accretion of disk material onto a forming star. Thus, if X-rays are produced in accretion flows one would expect to find that those same sources show ultraviolet excesses. We have calculated $U-V$ color excesses towards the H_2 detected sources (Table 5) by dereddening their U and V magnitudes and comparing the observed, dereddened $U-V$ colors with standard main-sequence colors (Johnson 1966). Using the photometry of GG Tau Aa and Ab from Ghez et al. (1997), we determined a value for the excess of each component of the northern binary. TW Hya, DoAr 21, and GG Tau Aa and GG Tau Ab all have significant excesses with $[U-V]_{\text{excess}} < -1.3$. LkCa 15 appears to have a smaller, but significant, ultraviolet excess. On this basis we conclude that each of these sources may still be undergoing active accretion and producing excess UV emission that could be responsible for stimulating some of the observed H_2 emission.

A closer look at the ultraviolet excesses from TW Hya and LkCa 15 suggests a possible dependence of $[U-V]_{\text{excess}}$ on the inclination angle of the disk. The nearly edge-on disk of LkCa 15 may absorb a significant fraction of the ultraviolet emission produced in the accretion process, just as suggested for the attenuation of its X-ray flux. On the other hand, TW Hya, which has been imaged and shown to be viewed nearly pole-on, produces the largest value of $[U-V]_{\text{excess}}$ of any of these four sources. Based on the shape of the H_2 emission line from DoAr 21, we inferred (Bary et al. 2002) the orientation of its disk to be more pole-on ($i > 55^\circ$) than that of LkCa 15; such an orientation is consistent with the larger value of $[U-V]_{\text{excess}}$ found for DoAr 21 than for LkCa 15. Due to the complexity of the GG Tau system, with both circumbinary and circumstellar material, we are unable to relate the $[U-V]_{\text{excess}}$ values for these stars to disk orientation in any meaningful manner. While our sample remains small so that we lack the statistical certainty that could prove the existence of a correlation between the strength of $[U-V]_{\text{excess}}$ and disk orientation, such a possible correlation is intriguing and consistent with the data presented.

6. Color-Color Diagrams

Near-infrared broad band photometry of YSOs previously has been used to identify sources that are likely candidates for harboring circumstellar disks. In this section, we examine infrared color-color diagrams to determine if there exists a correlation between the infrared excess, the implied presence of a circumstellar disk and the observed H_2 emission. $J-H$ vs. $H-K$ color-color diagrams of YSOs can be used to distinguish sources possessing infrared excesses from main-sequence stars. However, as described by Haisch et al. (2000), JHK observations do not sample long enough wavelengths to allow for unambiguous identification of sources that possess circumstellar disks. Lada et al. (2000) explain that the JHK near-infrared excess depends on the star/disk system (i.e., disk inclination, accretion rate, presence and size of holes in the inner disk) and also may be produced by emission from HII regions and reflection nebulae usually associated with star forming regions. L band observations, however, are much less sensitive to emission from HII regions and scattered light from reflection nebulae and will measure infrared excess emission from circumstellar disks independent of the star/disk system. Therefore, an infrared excess observed using $JHKL$ photometry can be characterized more confidently as being produced by a circumstellar disk. To this end, extensive L band surveys are being conducted to determine disk fractions in many nearby young star clusters (Lada et al. 2000; Haisch et al. 2000; Haisch et al. 2001a; Haisch et al. 2001b; Kenyon & Gómez 2001).

Using $JHKL$ observations made by Rydgren et al. (1976), Rucinski & Krautter (1983), Kenyon & Hartmann (1995), Strom et al. (1995), Coulson et al. (1998), and Calvet et al. (2002), we have plotted the TTS in our survey on JHK (Figure 3) and $JHKL$ (Figure 4) color-color diagrams. The solid main-sequence lines included on the diagrams are drawn from standard colors found in Koorneef (1983). With the exception of LkCa 15, none of the sources display unambiguous evidence of an infrared excess based solely upon the JHK

observations. However, the *JHKL* color-color diagram shows clear evidence of infrared excesses associated with GG Tau Aa, GG Tau Ab, LkCa 15, and TW Hya. All four of these have been observed to have other evidence of circumstellar material, either millimeter continuum observations and/or CO line emission. DoAr 21 shows only a marginal hint of a $K-L$ excess, as the error bar of its $K-L$ color overlaps with the interstellar reddening vector for a K1V star. Therefore, we conclude that DoAr 21 lacks strong evidence of a near-infrared excess, in good agreement with previous non-detections of millimeter continuum observations of this source (André et al. 1990; André & Montmerle 1994). More accurate K and L band photometry of DoAr 21 will determine its true position on the *JHKL* diagram and provide a more definitive conclusion as to the presence or absence of an infrared excess.

6.1. A Variety of Circumstellar H₂ Detections

Several detections of H₂ in the vicinity of young stellar objects have been made in recent years. As previously mentioned, *ISO* observations of Herbig Ae/Be stars and cTTS claim to have detected pure rotational emission from H₂ in the vicinity of these stars (Thi et al. 2001b). Ratios of the mid-infrared lines give temperatures of the emitting gas to be approximately ~ 100 K placing the gas in the outer regions of the disk at radii beyond 100 AU. These observations have yet to be confirmed and Richter et al. (2002) have called these interpretations into question. Herczeg et al. (2002) have detected far ultraviolet H₂ emission from the cTTS, TW Hya. They interpret this emission as produced by Lyman α pumping of H₂ molecules located within $0''.05$, or ~ 3 AU, of the source. In contrast to the pure rotational emission which may have been observed by *ISO*, the detections reported by Herczeg et al. (2002), Weintraub et al. (2000), Bary et al. (2002) and herein, represent the only detections of H₂ in the inner regions of TTS disks where planet formation may occur.

7. Conclusions

We have demonstrated that high-resolution, near-infrared spectroscopy of young stars can provide useful information about circumstellar gas around TTS. The discovery of ro-vibrational emission from quiescent H_2 towards GG Tau A and LkCa 15 adds to the increasing number of such observations (Weintraub et al. 2000; Bary et al. 2002). These data suggest that the gaseous component of circumstellar disks persists and may be substantial, even though other tracers of the gas may suggest otherwise. However, limited by the spatial resolution of our data, we have inferred the proximity of the emitting H_2 gas to the source from kinematic arguments, while further observations such as high-resolution narrow band images are needed to definitively identify the location of the H_2 emission. Spectral observations of other ro-vibrational H_2 emission lines are needed in order to determine a gas temperature and help confirm the excitation mechanism for the gas. Observations such as these will lead to a more complete understanding of the emission we have detected and the implications thereof to planet formation.

Special thanks to Tracy L. Huard for his assistance with data reduction techniques and discussions of color-color diagrams. Also, thanks to Phil Maloney, David Hollenbach, Didier Saumon, and Nuria Calvet for insightful discussions. Additional thanks to N. Calvet and Andrew Walsh for providing us with the L band photometry and G. Herczeg for providing us with *FUSE* continuum and line fluxes for TW Hya prior to publication. We also would like to thank KPNO staff members Hillary Mathis, Doug Williams, and Ken Hinkle for making our observing runs both productive and enjoyable. Thanks to Ginny Nickles for her assistance in making some of the observations reported herein. This work is supported by NASA grant NAG5-8295 to Vanderbilt University.

Table 1. WTTS and CTTS: H₂ Detections and Non-detections

Source	Class	Sp. ^a Type	K (mag)	H α ^b EW (Å)	log L _x ^c (ergs s ⁻¹)	Al (2.117 μm)	Al (2.121 μm)	H ₂ Line Flux (erg s ⁻¹ cm ⁻²)	H ₂ EW (Å)
IP Tau	cTTS	M0V	8.44	12.7	29.5	yes	yes	$< 1.2 \times 10^{-15}$...
IQ Tau	cTTS	M0.5V	8.16	7.7	...	yes	yes	$< 3.5 \times 10^{-15}$...
GG Tau A	cTTS	K7/M0.5V	7.3	40	29.4	yes	yes	$6.9 \pm 0.5 \times 10^{-15}$ ^d	0.10
V819 Tau	wTTS	K7V	7.97	3.2	30.2	yes	yes	$< 3.0 \times 10^{-15}$...
V836 Tau	wTTS	K7V	8.75	4.4	29.8	yes	yes	$< 9.4 \times 10^{-16}$...
GSS 29	wTTS	K7-MO ^e	8.19	...	30.4	yes	yes	$< 1.6 \times 10^{-15}$...
TW Hya	cTTS	K7V	7.37	220	30.3	...	yes	$1.0 \pm 0.1 \times 10^{-15}$ ^d	0.02
LkCa 15	cTTS	K5V	7.6	13	...	yes	yes	$1.7 \pm 0.2 \times 10^{-15}$ ^d	0.05
RXJ0516.3	wTTS	K4V	9.65 ^f	0.1	30.6	yes	... ^g	$< 1.8 \times 10^{-15}$...
SR 12	wTTS	K4-M2.5 ^e	8.1	4.5	30.4	yes	yes	$< 1.9 \times 10^{-15}$...
DoAr 25	wTTS	K3-M0 ^e	7.57	2.3	29.4	yes	yes	$< 2.2 \times 10^{-15}$...
DoAr 21	wTTS	K1V	6.13	0.8	31.2	yes	yes	$1.5 \pm 0.9 \times 10^{-14}$ ^d	0.06
HD 283572	wTTS	G5IV	6.53	1.6	31.2	no	no	$< 5.2 \times 10^{-15}$...
SU Aur	wTTS	G2III	5.86	3.5	30.5	no	no	$< 6.1 \times 10^{-15}$...
HD 34700	wTTS	G0V	7.45 ^f	no	no	$< 2.6 \times 10^{-15}$...
S1/GSS 35	wTTS	F2II	6.29	3.5	30.1	no	no	$< 3.8 \times 10^{-15}$...

^a Kenyon et al. (1998), Nürnberger et al. (1998), Wolk & Walter (1996), Hamann & Persson (1992), Chen et al. (1995), Leinert et al. (1993)

^b Herbig & Bell (1988), Kenyon et al. (1998), Bouvier & Appenzeller (1992), Webb et al. (1999), Allencar & Basri (2000)

^c Neuhauser et al. (1995), Casanova et al. (1995), Kamata et al. (1997), Magazzú et al. (1997)

^d The H₂ line flux value is extinction corrected. For stars with more than one value for A_v (Table 6), the larger A_v was used to obtain an upper limit.

^e Bouvier & Appenzeller (1992) list spectral types as peculiar and give two possible spectral types.

^f Estimated

^g Cannot be determined due to poor signal to noise in spectrum.

Table 2. Gas Mass Estimates

Source	hot H ₂ ^a (line emission) (M _⊙)	hot H ₂ ^b (LTE) (M _⊙)	warm H ₂ (17 & 28 μm) (M _⊙)	CO emission (M _⊙)	(sub)mm cont. (M _⊙)
GG Tau	1.5×10 ⁻¹⁰	2.8×10 ⁻⁸	3.6±2.0×10 ⁻³ ^c	1.3±0.1×10 ⁻³ ^d	0.116±0.052 ^e
LkCa 15	3.7×10 ⁻¹¹	7.0×10 ⁻⁹	8.6±4.3×10 ⁻³ ^f	...	0.18 ^g , 0.024 ^h , 0.033 ⁱ
DoAr 21	4.4×10 ⁻¹⁰	8.1×10 ⁻⁸	<0.0012 ^j
TW Hya	3.5×10 ⁻¹²	6.4×10 ⁻¹⁰	...	3.3 × 10 ⁻⁵ ^k	6.6 × 10 ⁻⁵ ^k

^a Calculated using equation (1)

^b Calculated using equation (2)

^c 17 and 28 μm line emission at ∼ 110 K from Thi et al. (1999)

^d ¹³CO line emission at ∼ 15 K from Dutrey et al. (1994)

^e 2.6 mm continuum emission at ∼ 35 K from Guilloteau et al. (1999)

^f Thi et al. (2001b)

^g Model dependent fit to SED from Chiang et al. (2000)

^h van Zadelhoff (2002)

ⁱ Duvert et al. (2000)

^j 1.3 mm continuum emission 3-σ upper limit from André et al. (1990)

^k Zuckerman et al. (1995)

Table 3. f values

Star	warm H ₂ ^a	CO ^b	(sub)mm ^c
GG Tau	10 ⁷	10 ⁷	10 ⁹
LkCa 15	10 ⁸	...	10 ^{9–10}
DoAr 21	≤10 ⁷
TW Hya	...	10 ⁷	10 ⁷

^a Found as a ratio of columns 4 and 2 from Table 2

^b Found as a ratio of columns 5 and 2 from Table 2

^c Found as a ratio of columns 6 and 2 from Table 2

Table 4. X-ray Model Parameters and Predicted Line Fluxes

Star	Observed $F_{v=1 \rightarrow 0 \ S(1)}$	$\log L_x$	Predicted X-ray Stimulated $F_{v=1 \rightarrow 0 \ S(1)}$ (ergs s ⁻¹ cm ⁻²)
TW Hya	$1.0 \pm 0.1 \times 10^{-15}$	30.3	$6.7 \times 10^{-16} \leq F_{v=1 \rightarrow 0 \ S(1)} \leq 5.0 \times 10^{-15}$
GG Tau A	$6.9 \pm 0.5 \times 10^{-15}$	29.4	$5.0 \times 10^{-16} \leq F_{v=1 \rightarrow 0 \ S(1)} \leq 5.0 \times 10^{-15}$
DoAr 21	$1.5 \pm 0.9 \times 10^{-14}$	31.2	$2.4 \times 10^{-17} \leq F_{v=1 \rightarrow 0 \ S(1)} \leq 2.4 \times 10^{-14}$
LkCa 15	$1.7 \pm 0.2 \times 10^{-15}$	29.4 ^a	$5.0 \times 10^{-16} \leq F_{v=1 \rightarrow 0 \ S(1)} \leq 5.0 \times 10^{-15}$

^a Assumed.

Table 5. Ultraviolet Excesses for H₂ Detections

Star	A _V (mag)	[U − V] _{observed}	[U − V] _{dereddened}	[U − V] _{excess}		References for A _V , U, V, Inclination Angle
TW Hya	0.1	0.86	0.73	−1.79	>85°	Herbst et al. (1994)
	0.25	0.86	0.81	−1.71		Herbst et al. (1994)
GG Tau Ab	3.02	2.73	1.13	−1.54	53° ^a	Ghez et al. (1997), White et al. (1999), Silber et al. (2000)
	3.38	2.73	0.94	−1.73		Ghez et al. (1997), White et al. (1999)
GG Tau Aa	0.46	1.42	1.18	−1.34	53° ^a	Ghez et al. (1997), White et al. (1999), Silber et al. (2000)
	0.98	1.42	0.90	−1.62		Ghez et al. (1997), White et al. (1999)
DoAr 21	6.2	3.82	0.53	−1.4	...	Herbst et al. (1994)
LkCa 15	0.64	1.75	1.41	−0.77	34° ± 14	Bouvier & Appenzeller (1992)
	0.64	2.21	1.87	−0.31		Hamann & Persson (1992)

^a Inclination angle for the circumbinary disk surrounding both GG Tau Aa and Ab.

REFERENCES

- Allencar, S. & Basri G. 2000, ApJ, 119, 1881
- André, Ph., Montmerle, T., Feigelson, E.D., & Steppe, H. 1990, A&A, 240, 321
- André, Ph. & Montmerle, T. 1994, ApJ, 420, 837
- Bary, J.S., Weintraub, D.A., & Kastner, J.H. 2002, ApJL, 576, L73
- Becklin, E.E., Mathews, K., Neugebauer, G., & Willner, S.P. 1978, ApJ, 220, 831
- Beckwith, S.V.W. & Sargent, A. 1993, ApJ, 402, 280
- Black, J.H. & van Dishoeck, E.F. 1987, ApJ, 322, 412
- Boss, A.P. 2000, ApJ, 536, L101
- Bouvier, J. & Appenzeller, I., 1992, A&AS, 92, 481
- Bouvier, J., Cabrit, S., Fernández, M., Martín, E.L., & Matthews, J.M. 1993, A&AS, 101, 485
- Calvet, N., D’Alessio, P., Hartmann, L., Wilner, D., Walsh, A., & Sitko, M. 2002, ApJ, 568, 1008
- Casanova, S., Montmerle, T., Feigelson, E., André, P. 1995, ApJ, 439, 752
- Chen, H., Myers, P.C., Ladd, E.F., & Wood, D.O.S. 1995, ApJ, 445, 377
- Chiang, E.I., Joungh, M.K., Creech-Eakman, M.J., Qi, C., Kessler, J.E., Blake, G.A., & van Dishoeck, E.F. 2001, ApJ, 547, 1077
- Choi, P.I. & Herbst, W. 1996, AJ, 111, 283
- Costa, V.M., Lago, M.T.V.T., Norci, L., & Meurs, E.J.A. 2000, A&A, 354, 621

- Coulson, I.M., Walther, D.M., & Dent, W.R.F. 1998, MNRAS, 296, 934
- Dougados, C., Cabrit, S., Lavalley, C., & Ménard, F. 2000, A&A, 357, L61
- Dutrey, A., Guilloteau, S., & Simon, M. 1994, A&A, 286, 149
- Duvert, G., Guilloteau, S., Ménard, Simon, M., Dutrey, A. 2000, A&A, 355, 165
- Edwards, S.E., Strom, S.E., Hartigan, P., Strom, K.E., Hillenbrand, L.A., Herbst, W.,
Attridge, J., Merrill, K.M., Probst, R., & Gatley, I. 1993, AJ, 106, 372
- Feigelson, E.D. & Montmerle, T. 1999, ARAA, 37, 363
- Ghez, A. M., White, R. J., & Simon, M. 1997, ApJ, 490, 353
- Glassgold, A.E., Feigelson, E.D., & Montmerle, T. 2000, Protostars & Planets IV, eds.
Mannings, V., Boss, A.P., & Russell, S.S., 429
- Gredel, R., & Dalgarno, A. 1995, ApJ, 446, 852
- Guilloteau, S., Dutrey, A., & Simon, M. 1999, A&A, 348, 570
- Haisch, K.E., Lada, E.A., & Lada, C.J. 2000, AJ, 120, 1396
- Haisch, K.E., Lada, E.A., & Lada, C.J. 2001a, AJ, 121, 2065
- Haisch, K.E., Lada, E.A., & Lada, C.J. 2001b, ApJ, 553, L153
- Hamann, F. & Persson, S.E. 1992, ApJ, 394, 628
- Herbig, G.H., & Bell, K.R. 1988, Third Catalog of Emission-Line Star of the Orion
Population (Santa Cruz: Lick Obs.)
- Herbst, T.M., Beckwith, S.V.W., Glindemann, A., Tacconi-Garman, L.E., Kroker, H. &
Krabbe, A. 1996, AJ, 111, 2403

- Herbst, W., Herbst, D.K., & Grossman, E.J. 1994, *AJ*, 108, 1906
- Herbst, W. 2002, *AAS* 200, 54.03
- Herczeg, G. J., Linsky, J. L., Valenti, J. A., Johns-Krull, C. M., & Wood, B. E. 2002, *ApJ*, 572, 310
- Hinkle, K., Wallace, L., & Livingston, W. 1995, “Infrared Atlas of the Arcturus Spectrum, 0.9 - 5.3 μm ,” *Astronomical Society of the Pacific* (San Francisco)
- Hinkle, K.H., Cuberly, R.W., Gaughan, N.A., Heynssens, J.B., Joyce, R.R., Ridgway, S.T., Schmitt, P., & Simmons, J.E. 1998, *SPIE*, 3354, 810-821
- Hollenbach, D., Yorke, H., & Johnstone, D. 2000, *Protostars & Planets IV*, eds. Mannings, V., Boss, A.P., & Russell, S.S., 401
- Johnson, H.L. 1966, *ARA&A*, 4, 193
- Kamata, Y., Koyama, K., Tsuboi, Y., Yamauchi, S. 1997, *PASJ*, 49, 461
- Kamazaki, T., Saito, M., Hirano, N., & Kawabe, R. 2001, *ApJ*, 548, 278
- Kastner, J.H., Huenemoerder, D.P., Schulz, N.S., Canizares, C.R. & Weintraub, D.A. 2002, *ApJ*, 567, 434
- Kenyon, S.J., Brown, D.I., Tout, C.A., & Berlind, P. 1998, *AJ*, 115, 2491
- Kenyon, S.J. & Gómez M. 2001, *AJ*, 121, 2673
- Kenyon, S.J. & Hartmann, L. 1995, *ApJS*, 101, 117
- Koorneef, J. 1983, *A&A*, 128, 84
- Krist, J.E., Stapelfeldt, K.R., Ménard, F., Padgett, D.L., & Burrows, C.J. 2000, *ApJ*, 538, 793

- Lada, C.J., Muench, A.A., Haisch, K.E., Lada, E.A., Alves, J.F., Tollestrup, E.V., & Willner, S.P. 2000, *AJ*, 120, 3162
- Leinert, Ch., Zinnecker, H., Weitzel, N., Christou, J., Ridgway, S.T., Jameson, R., Haas, M., & Lenzen, R. 1993, *A&A*, 278, 129
- Lissauer, J.J. 1993, *ARAA*, 31, 129
- Magazzú, A., Martin, E.L., Sterzik, M.F., Neuhäuser, R., Covino, E., & Alcalà, J.M., 1997, *A&AS*, 124, 449
- Maloney, P.R., Hollenbach, D.J., & Tielens, A.G.G.M. 1996, *ApJ*, 466, 561
- Mannings, V. & Sargent, A.I. 1997, *AJ*, 490, 792
- Neuhäuser, R., Sterzik, M., Schmitt, J., Wichmann, R., Krautter, J. 1995, *A&A*, 297, 391
- Nürnbergger, D., Brandner, W., Yorke, H. W., Zinnecker, H. 1998, *A&A*, 330, 549
- Osterloh, M. & Beckwith, S.V.W. 1995, *ApJ*, 439, 288
- Pollack, J. B., Hubickyj, O., Bodenheimer, P., Lissauer, J. J., Podolak, M., & Greenzweig, Y. 1996, *Icarus*, 124, 62
- Rebull, L. M. 2001, *AJ*, 121, 1676
- Richter, M. J., Jaffe, D. T., Blake, G. A., & Lacy, J. H., 2002, *ApJ*, 572, L161
- Rucinski, S. M. & Krautter, J. 1983, *A&A*, 121, 217
- Rydgren, A.E., Strom, S.E., & Strom, K.M. 1976, *ApJS*, 30, 307
- Safier, P.N. 1995, *ApJ*, 444, 818
- Shevchenko, V.S. & Herbst, W. 1998, *AJ*, 116, 1419

- Silber, J., Gledhill, T., Duchene, G., & Ménard, F. 2000, *ApJ*, 536, L89
- Skrutskie, M.F., Snell, R.L., Strom, K.M., Strom, S.E., Edwards, S., Fukui, Y., Mizuno, A., Hayashi, M., & Ohashi, N. 1993, *ApJ*, 409, 422
- Stassun, K.G., Mathieu, R.D., Mazeh, T., & Vrba, F.J. 1999, *AJ*, 117, 2941
- Strom, K.M., Kepner, J., & Strom, S.E. 1995, *ApJ*, 438, 813
- Tanaka, M., Hasegawa, T., Hayashi, S.S., Brand, P.W.J.L., & Gatley, I. 1989, *ApJ*, 336, 207
- Thi, W., van Dishoeck, E.F., Blake, G.A., van Zadelhoff, G., & Hogerheijde, M.R. 1999, *ApJ*, 521, L63
- Thi, W. et al. 2001a, *Nature*, 409, 60
- Thi, W., van Dishoeck, E.F., Blake, G.A., van Zadelhoff, G.J., Horn, J., Becklin, E.E., Mannings, V., Sargent, A.I., van den Ancker, M.E., & Natta, A., Kessler, J. 2001b, *ApJ*, 561, 1074
- Tine, S., Lepp, S., Gredel, R., & Dalgarno, A. 1997, *ApJ*, 481, 282
- Turner, J., Kirby-Docken, K., & Dalgarno, A. 1977, *ApJS*, 35, 281
- van Zadelhoff, G.J. 2002, PhD Thesis, “Shaping Disks: A Radiative Transfer and Gas Abundance Study of Circumstellar Matter”, University of Leiden p.65
- Wallace, L., & Hinkle, K. 1996, *ApJS*, 107, 312
- Webb, R.A., Zuckerman, B., Patience, J., White, R.J., Schwartz, M.J., McCarthy, C., & Platais, I. 1999, *ApJ*, 512, L63
- Weinberger, A.J., Becklin, E.E., Schneider, G., Chiang, E.I., Lowrance, P.J., Silverstone, M., Zuckerman, B., Hines, D.C., & Smith, B.A. 2002, *ApJ*, 566, 409

- Weintraub, D. A., Kastner, J. H., & Bary, J.S. 2000, ApJ, 541, 767
- Weintraub, D. A., Kastner, J. H., Zuckerman, B., & Gatley, I. 1992, ApJ, 391, 784
- Weintraub, D.A., Masson, C.R., & Zuckerman, B. 1989, ApJ, 344, 915
- Weintraub, D. A., Sandell, G., & Duncan, W. D. 1989, ApJ, 340, L69
- White, R.J., Ghez, A.M., Reid, I.N., & Shultz, G. 1999, ApJ, 520, 811
- Willing, B.A., Bontemps, S., Schuler, R.E., Greene, T.P., & André, P. 2001, ApJ, 551, 357
- Wilner, D.J., Ho, P.T.P., Kastner, J.H., & Rodriguez, L.F. 2000, ApJ, 534L, L101
- Wolk, S.J. & Walter, F.M. 1996, AJ, 111, 2066
- Yan, M., Sadeghpour, H.R., & Dalgarno, A. 1998, ApJ, 496, 1044
- Zuckerman, B., Forveille, T., & Kastner, J. H. 1995, Nature, 373, 494

Figure Captions

Fig. 1.— Full spectra for target stars and calibration sources. The spectra are not shifted in wavelength or corrected for telluric or photospheric absorptions. Due to instrument problems during our Taurus-Auriga observing run, a few spectra are shifted in wavelength as evidenced by misaligned telluric absorption features. However, a wavelength calibration was performed for each night and in some case for individual observations when deemed necessary to correct this systemic error. Note an uncorrected bad pixel in the spectra of S1 near $2.1176\ \mu\text{m}$.

Fig. 2.— Spectra containing the emission lines associated with the $v = 1 \rightarrow 0$ S(1) transition

at $2.12183\ \mu\text{m}$. Shifted to the systemic velocity for each source, the emission is nearly centered at the rest velocities of the sources, to within errors.

Fig. 3.— *JHK* color-color diagram of the four TTS detected in emission at $2.12183\ \mu\text{m}$. Only the interstellar reddening vectors for K1V and K7V stars are plotted. Since the difference between the K5V, K7V, and M0V vectors are barely the thickness of the plotted line, vectors corresponding to the K5V and M0V spectral types are not plotted and can be estimated from the K7V line. According to these vectors, only LkCa 15 shows clear evidence of a shift due to circumstellar reddening, while GG Tau Aa and GG Tau Ab show only a marginal shift and remain within errors of the reddening vectors. The crosses correspond to $\pm 1\text{-}\sigma$ errors in photometry.

Fig. 4.— *JHKL* color-color diagram of the four TTS detected in emission at $2.12183\ \mu\text{m}$. Only the interstellar reddening vectors for K1V and K7V stars are plotted. All sources, with the exception of DoAr 21 show clear evidence of circumstellar material with substantial shifts from the plotted interstellar reddening vectors. DoAr 21 is shifted marginally but its position on the diagram remains, within errors, consistent with interstellar reddening along the K1V reddening vector. The crosses correspond to $\pm 1\text{-}\sigma$ errors in photometry.

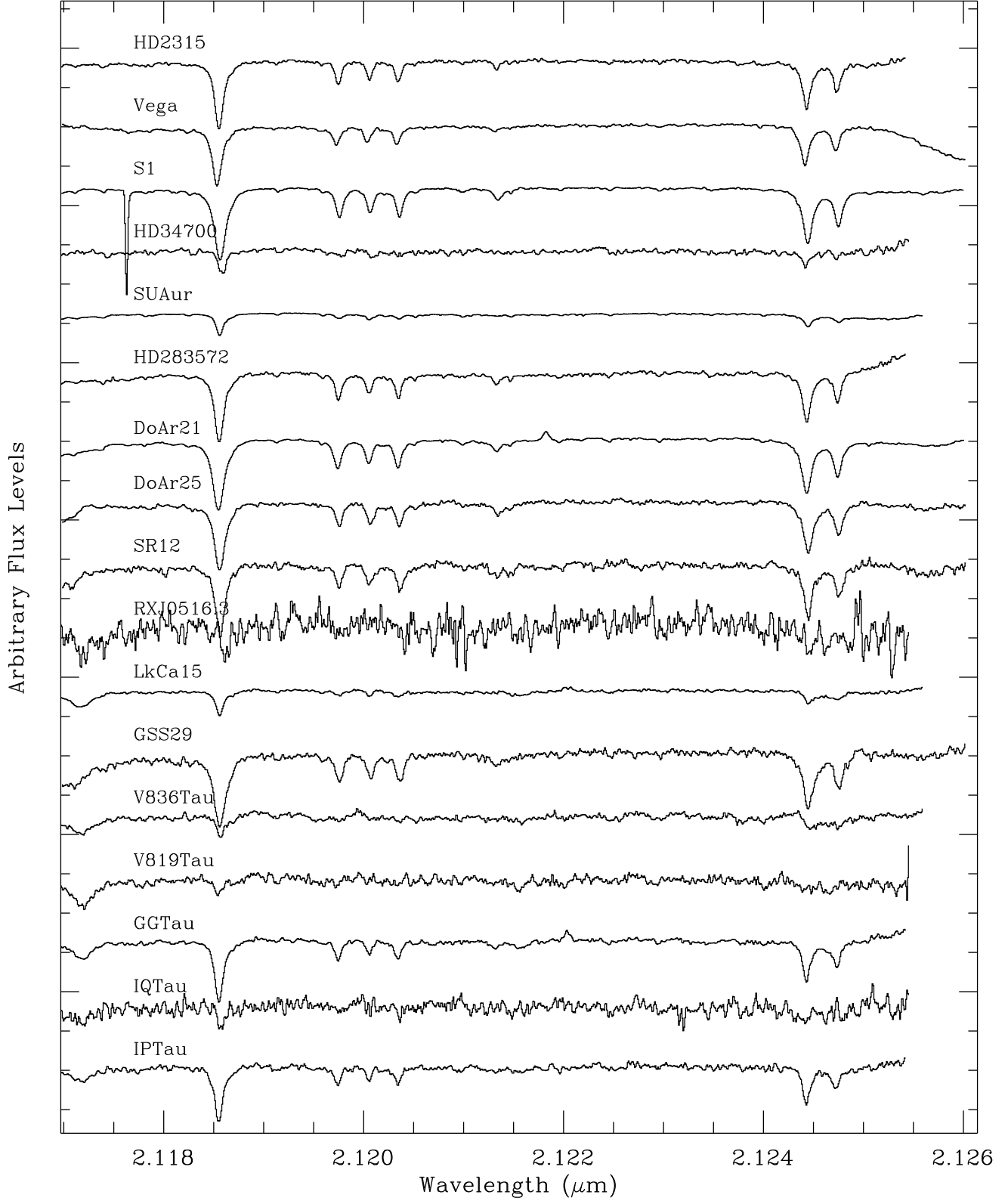


Fig. 1.— Source spectra

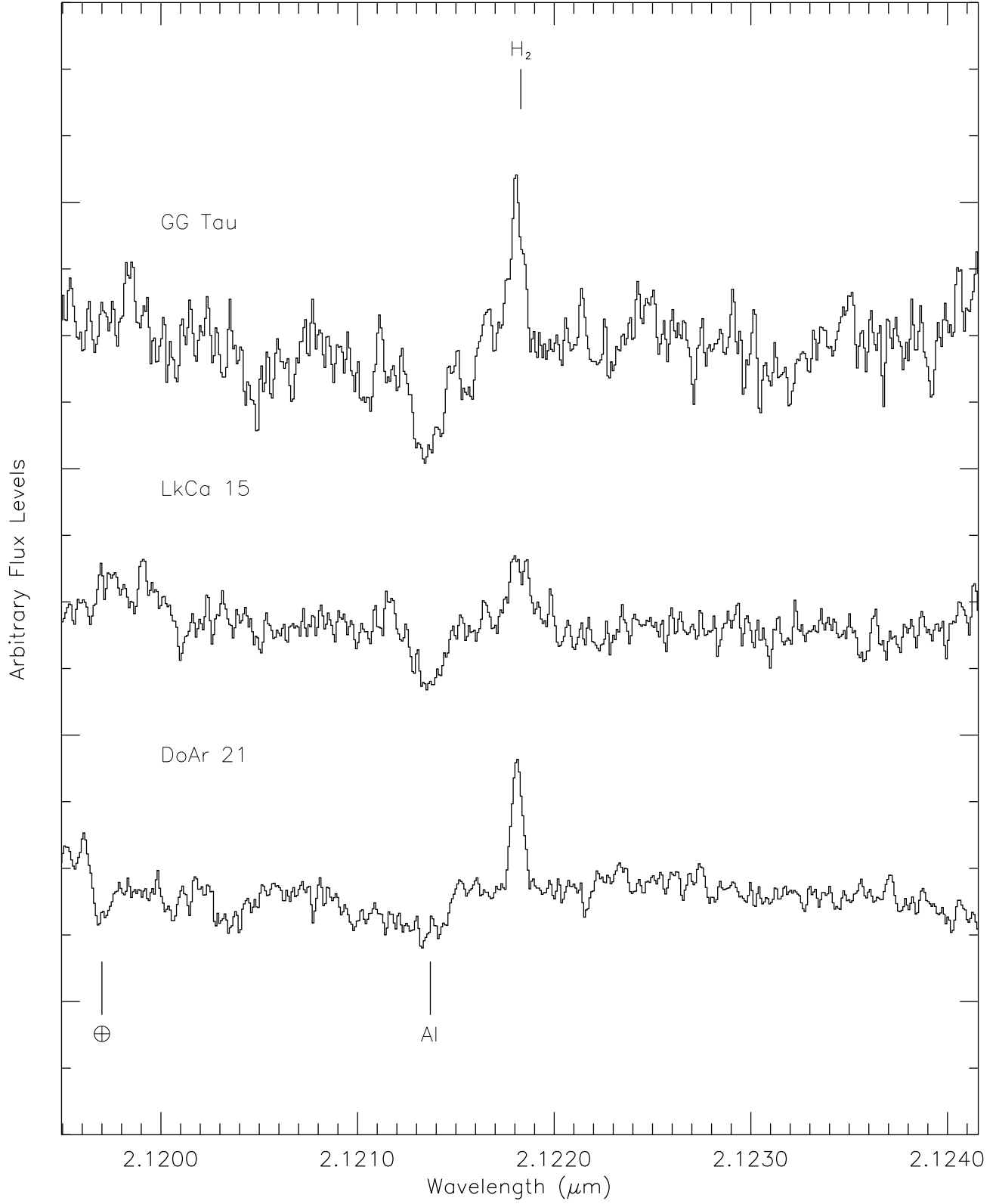


Fig. 2.— Emission spectra

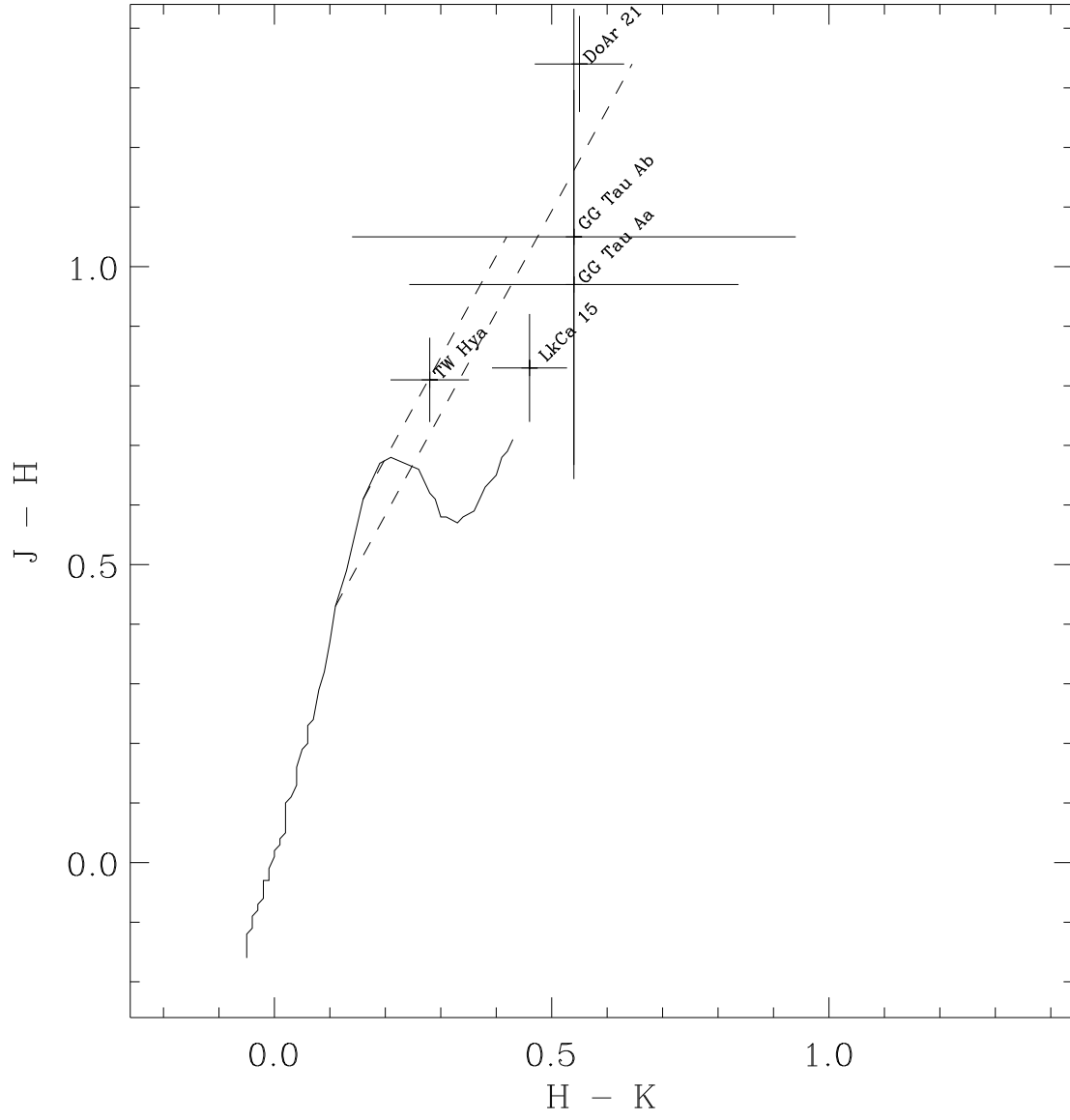


Fig. 3.— *JHK* Color-Color Diagram

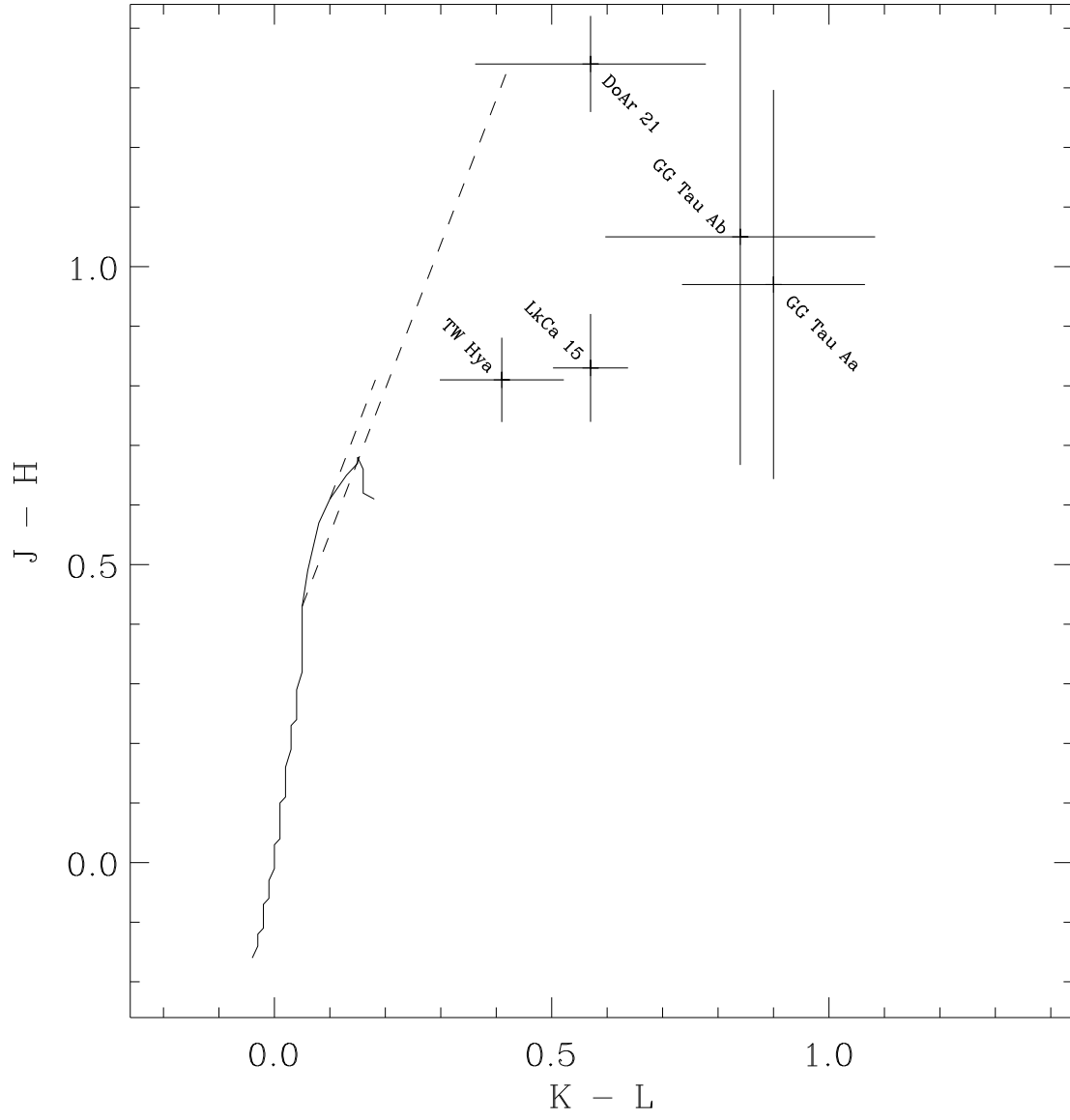


Fig. 4.— *JHKL* Color-Color Diagram